

# The Hydrated Proton at the Water Liquid/Vapor Interface

Matt K. Petersen,<sup>†</sup> Srinivasan S. Iyengar,<sup>‡</sup> Tyler J. F. Day,<sup>†</sup> and Gregory A. Voth<sup>\*,†</sup>

Department of Chemistry and Henry Eyring Center for Theoretical Chemistry, University of Utah, 315 S. 1400 E. Rm. 2020, Salt Lake City, Utah 84112-0850, and Department of Chemistry and Department of Physics, Indiana University, 800 E. Kirkwood Avenue, Bloomington, Indiana 47405

Received: July 23, 2004; In Final Form: August 22, 2004

The hydrated proton was studied at the water liquid/vapor interface using the multistate empirical valence bond (MS-EVB) methodology, which enables the migration of the excess proton to and about the interface through the fluctuating bond topology described by the Grotthuss shuttle mechanism. It was found in our model that the hydrated excess proton displays a marked preference for water liquid/vapor interfaces. The resulting stable surface structures can be explained through an examination of the bond network formed between the water/proton moiety and solvating water. These results suggest the excess proton can effectively behave as an amphiphile, displaying both hydrophobic and hydrophilic character.

In this communication, interesting new results are reported for the excess proton at the water liquid/vapor interface. These results are at odds with the conventional concepts of ionic solvation and have their origin in the strong solvation asymmetry of the hydronium cation. In particular, the water liquid/vapor interface for the  $\text{H}^+(\text{H}_2\text{O})_{1000} \text{Cl}^-$  system, constituting a “slab”<sup>1,2</sup> geometry for the water molecules and the two ions, was studied via molecular dynamics (MD) simulations using rectangular periodic boundaries at 300 K and a constant volume of dimensions  $31.2 \times 31.2 \times 75.0 \text{ \AA}^3$ . Starting configurations were generated from a constant temperature trajectory after an initial equilibration of 500 ps with the Nose–Hoover thermostat. Ten independent microcanonical trajectories were then collected, for a total of 2.5 ns of simulation time, using MD simulations performed with the MS-EVB2 model,<sup>3,4</sup> and the Ewald summation method was implemented for all electrostatic interactions. The MS-EVB2 model has been successfully used to treat proton transport in bulk liquids and several biological systems.<sup>5–8</sup> The important distinction in this approach is that the definition of the protonated species can change during the dynamical process; that is, the proton can hop along an optimal conformation of water molecules consistent with the Grotthuss mechanism of proton transfer.<sup>9,10</sup> As a result of the present simulation, it was found that the proton was preferentially distributed on the surface of the water/vacuum interface. This surface localization of the hydronium was also evident for a simple “classical” model of the cation, that is, one which is unable to participate in Grotthuss hopping (see Figure 1). The orientation of the hydrated proton is such that the lone-pair side was directed away from the aqueous portion of the interface. A representative structure from an MS-EVB2 trajectory is shown in Figure 2 with the hydronium (orange) located at the interface and the counterion, in this case chloride (green), visible several molecules below the surface. Although not discussed here in detail, it is worth noting that the simulated chloride ion’s radial distribution, diffusion, and coordination are in agreement with previously published values.<sup>11,12</sup>

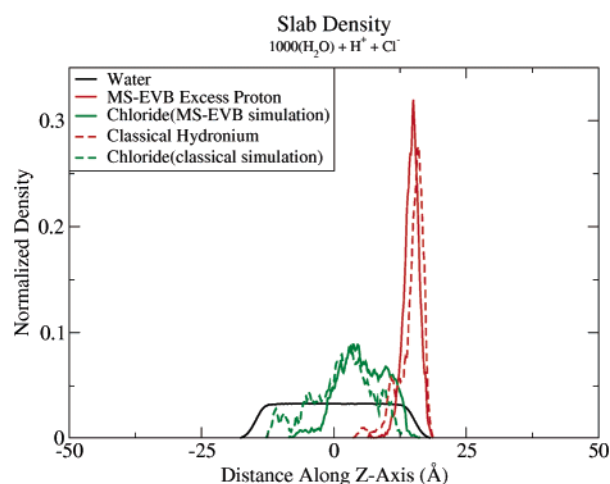


**Figure 1.** Individually normalized molecular densities for the  $\text{H}^+\text{Cl}^-(\text{H}_2\text{O})_{1000}$  water slab: water (black); MS-EVB2 excess proton (solid red); classical hydronium (dashed red); chloride counterion for the MS-EVB2 simulation (solid green); chloride counterion in the classical hydronium simulation (dashed green). The surface of the water slab is normal with the  $z$ -axis along which all densities were calculated.

While the phenomenon of the “surface” excess proton observed in this work is perhaps counterintuitive, it can be explained on the basis of the hydrogen bonding pattern of the protonated species with adjacent solvating water molecules. A water molecule has, on average, just less than four hydrogen bonds in liquid water. One each is donated to other waters from its covalently bound hydrogens, while two hydrogen bonds are donated to the lone pairs on its oxygen atom. When the water molecule forms a covalent bond with an excess proton to form hydronium, it also gains a net positive charge. The coordination also changes from the approximately four hydrogen bonds of the water molecule to three very strongly solvated waters on one side of the hydronium cation (forming the so-called “Eigen cation”,  $\text{H}_3\text{O}_4^+$ ). On average, the center of positive charge in the hydronium resides on the oxygen atom. Hence, while the hydrogen atoms in the hydronium retain their hydrogen bonds to the oxygen of neighboring water molecules, the oxygen is unable to support a fourth full hydrogen bond being donated to

\* Corresponding author. E-mail: voth@chemistry.utah.edu.

<sup>†</sup> University of Utah.

<sup>‡</sup> Indiana University.

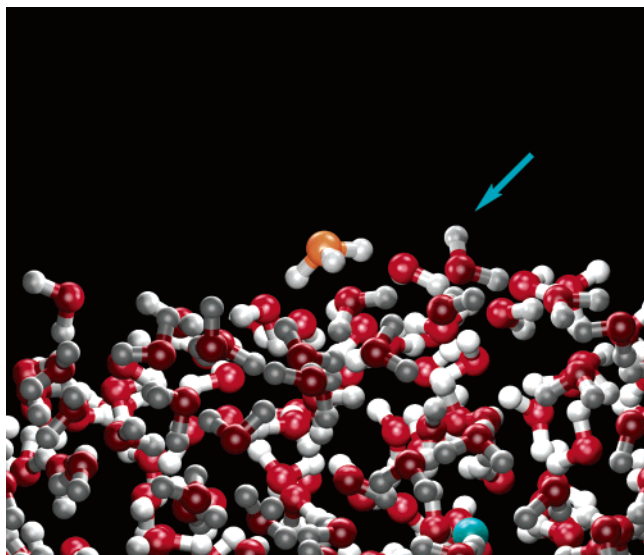


**Figure 2.** Representative structure from the MS-EVB2 simulation of the two-dimensional slab of water molecules. The vertical direction defines the liquid/vapor interface, across which the so-called dangling O–H bonds of the water protrude (arrow). The hydronium ion on the surface is highlighted in orange, with its lone-pair side pointing outward away from the liquid interface. The negative chloride counterion is seen a few solvation shells below in green.

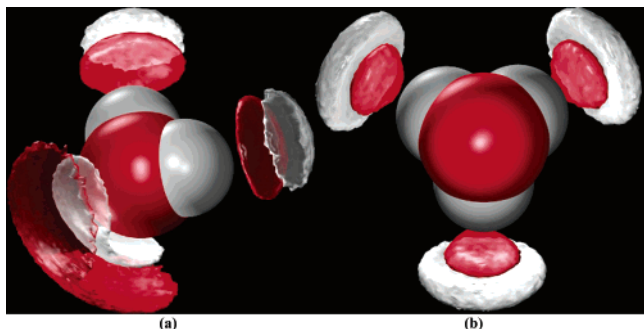


**Figure 3.** (a) The isodensity surface for the oxygen (red) and hydrogen (white) atoms of water molecules solvating a central water molecule in a bulk water simulation. The surfaces correspond to points containing 4 times the average atomic densities. (b) The isodensity surface for the oxygen (red) and hydrogen (white) atoms of water molecules solvating the hydronium cation in a bulk phase MS-EVB2 simulation. The surfaces again correspond to points containing 4 times the average atomic densities. Note the reduced density on the lone-pair side of the hydronium molecule.

it by a neighboring water molecule. This results in a very strong solvation asymmetry of the hydronium cation due to its molecular structure, although it is still a positively charged ion.

This solvation asymmetry is depicted in Figure 3 in which panel a depicts an isodensity surface of solvating water molecules surrounding a solute water molecule calculated from a bulk water MD simulation. The oxygen (red) and hydrogen (white) surfaces represent those points that on average contain densities greater than 4 times the average atomic densities. The density for those solvating molecules, which are accepting hydrogen bonds, is clearly localized beneath the water molecule's hydrogen atoms. Those molecules donating hydrogen bonds are likewise restricted, albeit less localized, to the region above the solvated molecule's oxygen atom. Panel b depicts similarly defined isodensity surfaces for solvating water molecules surrounding the solute hydronium molecule from a bulk water MS-EVB2 simulation of the hydrated proton. The reduction in coordination seems unmistakable. It should be noted

that while the MS-EVB2 model may somewhat overexpress the water density reduction on the lone-pair side of the hydronium cation, the strong directional solvation asymmetry of this cation is well-described by the model and is, in fact, present in even a classical model of the hydronium cation in which Grotthuss shuttling is not allowed.

Clearly, the hydronium ion is highly anisotropic from the perspective of the surrounding solvent. In turn, this anisotropy may lead to an enhanced ordering of the water molecules in the vicinity of the hydronium, resulting in an unfavorable decrease in entropy which is seemingly consistent with the hydrophobic effect. Interestingly, however, if the hydronium can migrate to a water/vapor (or other) interface, with the lone-pair side of the oxygen atom pointing outward, it can still retain its three strong hydrogen bonds while avoiding to some degree the disturbance of the water network. Therefore, the protonated species is apparently more stable at the interface with its oxygen atom pointed outward, as seen in Figure 2. We have also found that this is also the case for many protonated water clusters.<sup>13</sup>

It should be noted that calculations have recently been carried out by Dang<sup>24</sup> of the potential of mean force (PMF) to reversibly move a classical hydronium (with no Grotthuss shuttling) across the water/air interface. These calculations yielded no substantial minimum in the PMF at the interface. However, given that the classical hydronium in these latter simulations drags water molecules with it into the gas phase during the MD sampling to calculate the PMF, the relationship with the present results seems unclear.

The surface preference of the solvated proton apparent in our computational study seems consistent with the experimental findings of Shen<sup>14,15</sup> and Shultz and co-workers<sup>16</sup> who performed sum-frequency vibrational spectroscopy (SFVS) experiments on liquid water/vapor interfaces. Shen and co-workers found that the SFVS spectrum of the water liquid/vapor interface demonstrates a sharp peak at  $3700\text{ cm}^{-1}$  corresponding to dangling O–H bonds on the water surface, an example of which is shown by the arrow in Figure 2. The intensity of this peak substantially diminishes with increasing acid concentration. These results led Shen and co-workers to the conjecture that the acid concentration is greater near the surface, resulting in increased ordering of the hydrogen bond network at the interface. Our results and the qualitative reasoning that we provide here are consistent with these experimental findings.

In an attempt to quantify the dangling O–H bond effect, we have calculated the radial distribution of these dangling bonds as a function of distance from both the excess proton and the chloride counterion, as well as from the water oxygens (Figure 4). All water molecules  $>10\text{ \AA}$  from the center of mass of the slab in the  $z$ -direction were inspected for dangling bonds. Any covalent O–H bond for which the hydrogen atom was further from the  $z$ -origin than the bound oxygen and was not within  $2.7\text{ \AA}$  of another oxygen was considered dangling. A radial distribution parallel to the surface of the slab was constructed for each ion and all of the water molecules. From these results, a significant negative association is seen between the hydronium oxygen and the dangling bonds and apparently a positive association is seen for the chloride. For comparison, it may be noted that our interface has an acid mole fraction of  $\sim 0.1\text{ mol \%}$ . Shen and co-workers found a significant reduction in the dangling O–H bond concentration as the acid concentration was increased. Their experimental dangling O–H bond concentration became negligible as the acid concentration approached  $6\text{ mol \%}$ . The results presented here are primarily “local” results within the proximity of the ions at a much lower effective concentra-

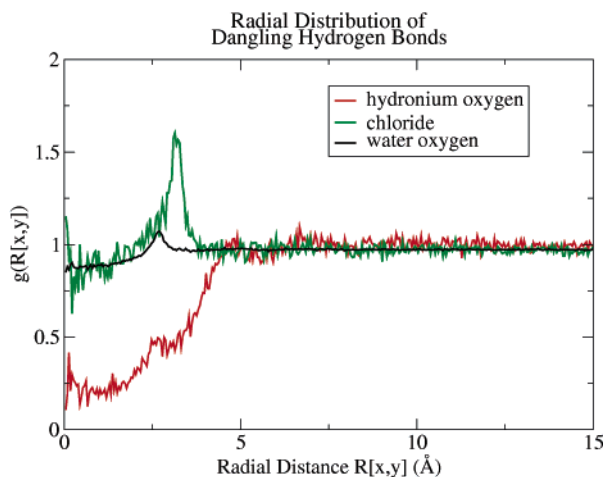


**Figure 4.** The chloride counterion (green), MS-EVB2 hydronium oxygen (red), and water oxygen (black) ( $x,y$ ) radial distribution of the associated water dangling O–H bonds.

tion, so it would be expected that a higher concentration will be required in the MD simulations in order to make direct contact with experiment. This will be the topic of future research.

Interesting MD results have been found for other ions solvated in both clusters and at the water liquid/vapor interface.<sup>17–23</sup> Ionic charge and size appear to have a striking influence on the behavior of solvated ions near the interface. For example, positive ions such as  $\text{Na}^+$  are seen to prefer the interior,<sup>18,23</sup> while negative ions may prefer the surface or the interior, apparently based primarily on their size.<sup>17,18,20,23</sup> The current explanation of this effect is based on the symmetry of the solvation shell for a positive ion, which is absent for the negative ion. Furthermore, the presence of a negative counterion that prefers the surface over the interior may force the positive ion to also approach the surface.<sup>23</sup> Our results, however, seem to differ from these, since the hydronium is positively charged but remains on the surface rather than the interior.

It clearly seems that the hydrogen bonding and lone-pair directionality of the  $\text{H}_3\text{O}^+$  ion fundamentally differentiate it from other simple monovalent cations such as  $\text{Na}^+$  and  $\text{Li}^+$ . Rather, our results suggest that the hydronium ion has a “hydrophobic” region on the lone-pair side of the oxygen. This is a result of the strong directional asymmetry of solvation of the hydronium cation, so that water molecules are effectively “excluded” from the volume on the side of the hydronium oxygen lone pair, especially in comparison to the strong hydrogen bonds with three waters on the opposite side. One can therefore define a “directional hydrophobicity” for the hydronium ion, which is typical of amphiphilic molecules. Indeed, it has been demonstrated through computer simulation,<sup>25</sup> as well as SFVS,<sup>14</sup> that the liquid/vapor interfaces of amphiphilic solutions such as methanol and methanol/water mixtures are more ordered than the bulk. A gradient of increasing methanol concentration toward the liquid interface exists in water/methanol solutions with a

preferential orientation of the methyl group at the liquid interface. The behavior seen in our MD simulations of the excess proton in water is quite analogous to the amphiphilic nature of methanol, which has a hydrophobic region around the methyl group and a polar hydrophilic region around the hydroxyl group. Our simulations would also seem to suggest the existence of a negative pH gradient toward the water liquid/vapor interface. We believe this finding may have significant implications for excess protons in mixed hydrophobic/hydrophilic environments such as proteins, lipid bilayers, liquid/vapor interfaces, water/amphiphile solutions, and polymer membranes, as well as for acidified atmospheric aerosols.

**Note Added in Proof.** Results for a smaller system of 125 water molecules plus an excess proton and chloride counterion were first presented at the August 2002 National American Chemical Society Meeting in Boston, MA, containing the same qualitative conclusions as described in the present Letter.

**Acknowledgment.** This research was supported by the National Science Foundation (CHE-0317132).

## References and Notes

- (1) Wilson, M. A.; Pohorille, A. *J. Chem. Phys.* **1991**, *95*, 6005.
- (2) Schweighofer, K. J.; Benjamin, I. *Chem. Phys. Lett.* **1993**, *202*, 379.
- (3) Schmitt, U. W.; Voth, G. A. *J. Chem. Phys.* **1999**, *111*, 9361.
- (4) Day, T. J. F.; Soudachov, A. V.; Cuma, M.; Schmidt, U. W.; Voth, G. A. *J. Chem. Phys.* **2002**, *117*, 5839.
- (5) Smondyrev, A. M.; Voth, G. A. *Biophys. J.* **2002**, *82*, 1460.
- (6) Smondyrev, A. M.; Voth, G. A. *Biophys. J.* **2002**, *83*, 1987.
- (7) Wu, Y.; Voth, G. A. *Biophys. J.* **2003**, *85*, 864.
- (8) Ilan, B.; Tajkhorshid, E.; Schulten, K.; Voth, G. A. *Biophys. J.* **2004**, *86*, 131A.
- (9) Agmon, N. *Chem. Phys. Lett.* **1995**, *244*, 456.
- (10) Bell, R. P. *The Proton in Chemistry*; Cornell University Press: Ithaca, NY, 1973.
- (11) Lyubartsev, A. P.; Laaksonen, A. *J. Phys. Chem.* **1996**, *100*, 16410.
- (12) Dang, L. X.; Smith, E. D. *J. Chem. Phys.* **1993**, *99*, 6950.
- (13) Burnham, C. J.; Iyengar, S. S.; Petersen, M. K.; Day, T. J. F.; Voth, G. A. To be submitted for publication.
- (14) Miranda, P. B.; Shen, Y. R. *J. Phys. Chem. B* **1999**, *103*, 3292.
- (15) Raduge, C.; Pflumio, V.; Shen, Y. R. *Chem. Phys. Lett.* **1997**, *274*, 140.
- (16) Shultz, M. J.; Schnitzer, C.; Simonelli, D.; Baldelli, S. *Int. Rev. Phys. Chem.* **2002**, *19*, 123.
- (17) Yeh, I.-C.; Perera, L.; Berkowitz, M. L. *Chem. Phys. Lett.* **1997**, *264*, 31.
- (18) Tobias, D. J.; Jungwirth, P.; Parrinello, M. *J. Chem. Phys.* **2001**, *114*, 7036.
- (19) Dang, L. X.; Chang, T.-M. *J. Phys. Chem. B* **2002**, *106*, 235.
- (20) Stuart, S. J.; Berne, B. J. *J. Phys. Chem. A* **1999**, *103*, 10300.
- (21) Egorov, A. V.; Brodskaya, E. N.; Laaksonen, A. *J. Chem. Phys.* **2003**, *118*, 6380.
- (22) Knipping, E. M.; Lakin, M. J.; Foster, K. L.; Jungwirth, P.; Tobias, D. J.; Gerber, R. B.; Daddub, D.; Finlayson-Pitts, B. J. *Science* **2000**, *288*, 301.
- (23) Garrett, B. C. *Science* **2004**, *303*, 1164.
- (24) Dang, L. X. *J. Chem. Phys.* **2003**, *119*, 6351.
- (25) Matsumoto, M.; Kataoka, Y. *J. Chem. Phys.* **1989**, *90*, 2398.
- (26) Illustration created with the visualization package VMD; Humphrey, W.; Dalke, A.; Schulten, K. *J. Mol. Graphics* **1996**, *14*, 33.
- (27) Illustrations rendered with Raster3D; Merritt, E. A.; Murphy, M. E. P. *Acta Crystallogr.* **1994**, *D50*, 869.